Investigation of kinetic compensation effect in lignocellulosic biomass torrefaction: Kinetic and thermodynamic analyses

Zhiqing Zhang [a,#], Hanqi Duan [a,#], Youjun Zhang [b], Xiaojuan Guo [c], Xi Yu [d], Xingguang Zhang [b], Md. Maksudur Rahman [e], Junmeng Cai [a,*]

[a] Biomass Energy Engineering Research Center, School of Agriculture and Biology, Shanghai Jiao Tong University, 800 Dongchuan Road, Shanghai 200240, People's Republic of China

[b] College of Chemical Engineering, Nanjing Forestry University, 159 Longpan Road, Nanjing 210037, People's Republic of China

[c] School of Chemical Engineering and Energy Technology, Dongguan University of Technology, 1 Daxue Road, Songshan Lake, Dongguan 523808, Guangdong Province, People's Republic of China

[d] Energy & Bioproducts Research Institute (EBRI), School of Engineering & Applied Science, Aston University, Aston Triangle, Birmingham B4 7ET, United Kingdom

[e] Discipline of Chemical Engineering, Western Australian School of Mines: Minerals, Energy and Chemical Engineering, Curtin University, GPO Box U1987, Perth, WA 6845, Australia

[#] Zhiqing Zhang and Hanqi Duan contributed equally to this work.

* Corresponding author. Junmeng Cai. Tel.: +86-21-34206624; E-mail: jmcai@sjtu.edu.cn; Website: http://biofuels.sjtu.edu.cn.

Abstract

The kinetic compensation effect between the activation energy and the pre-exponential factor has extensively existed in the thermochemical conversion processes of lignocellulosic biomass. The research on the kinetic compensation effect in lignocellulosic biomass torrefaction has been insufficient yet. The torrefaction of the pinewood sample was experimentally investigated by thermogravimetric analysis (TGA) at four isothermal temperatures of 220, 250, 265 and 280 °C. The reaction order model was used to analyze the isothermal torrefaction kinetics of lignocellulosic biomass, and the results showed that many sets of activation energy and pre-exponential factor could describe the experimental data at each temperature equally well and they excellently satisfied the kinetic compensation effect relationship. The linear regression lines of the kinetic compensation effect points at different temperatures intersected at one point, whose values corresponded to the obtained optimal kinetic parameters. A kinetic-compensation-effect-based method was developed and verified to determine the kinetic parameters of isothermal biomass torrefaction. Based on the optimal kinetic parameters, the thermodynamic parameters (including Gibbs free energy, enthalpy, and entropy) of biomass torrefaction processes at various temperatures were calculated and analyzed.

Keywords: Biomass torrefaction; Isothermal kinetics; Kinetic compensation effect; Thermodynamic analysis.

Graphical abstract

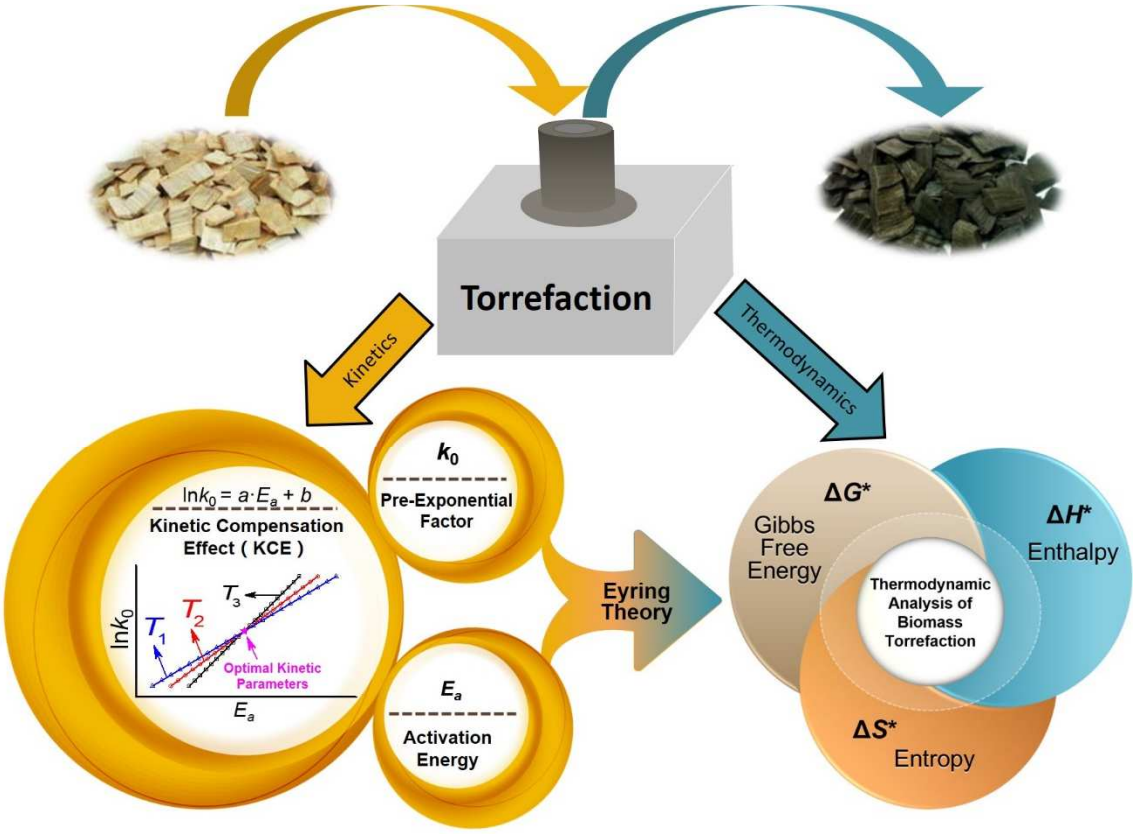

Highlights

- Isothermal torrefaction kinetics of biomass was experimentally investigated by TGA.
- Kinetic compensation effect (KCE) was found between kinetic parameters.
- A KCE-based-method to determine kinetic parameters of torrefaction was developed.
- The thermodynamic parameters (ΔG^*, ΔH^*, and ΔS^*) were calculated and discussed.

1 Introduction

Raw biomass, containing high moisture content, low calorific value, and hygroscopic nature, as a consequence, collection, processing, storage and transportation of biomass is a matter of concern. At the same time, the thermochemical conversion performance of raw biomass adversely affected by its lower-thermal quality [1]. The direct use of raw biomass is limited by logistical, economic, or technical factors; therefore, pretreatment may be required [2, 3]. As one of the most recognized thermal pretreatment technologies, torrefaction can enhance the biomass thermochemical conversion utilization by improving its physical and chemical properties [4, 5]. Torrefaction, as a mild pyrolysis process, is carried out in a temperature range of 200 to 300 °C in the absence of oxygen. With the removal of water and light volatiles containing most of the oxygen in biomass, and the partial destruction of the fibrous structure of the original biomass material, torrefaction can reduce the moisture content of biomass and increase its energy density, make its properties changing from hygroscopic to hydrophobic, and improve its grindability [6, 7].

The design of a biomass torrefaction system requires hydrodynamic and thermochemical performance simulation which involves information about mass and heat transfer as well as chemical reaction kinetics [8]. Kinetic analysis of biomass torrefaction can generate the values of activation energy and pre-exponential factor, which are very important and can certainly be used in estimating conversion and conversion rates of biomass torrefaction at various temperatures [9]. Therefore, A comprehensive understanding of biomass torrefaction kinetics is essential to the design and optimization of a torrefaction system and its scale-up for industrial applications [10, 11].

In general, the reaction rate constant of a solid-state reaction can be described by the Arrhenius law [12]:

$$k = k_0 \exp\left(-\frac{E_a}{R \cdot (T + 273.15)}\right) \quad (1)$$

where k is the reaction rate constant (s^{-1}), k_0 is the pre-exponential factor (s^{-1}), E_a is the activation energy (J mol^{-1}), R is the universal gas constant (8.3145 J mol^{-1} $°C^{-1}$), and T is the temperature (°C). The Arrhenius law is widely used because it is simple and can correctly describe the exponential dependence of endothermic reaction rate on temperature [13]. For most chemical reactions, the effect of an increase of activation energy, expected to decrease the reaction rate at a particular temperature, is partially or entirely offset by a compensatory rise in pre-exponential factor, which is referred to the kinetic compensation effect [13]:

$$\ln k_0 = a \cdot E_a + b \quad (2)$$

where a and b are compensation effect constants, a is the slope (mol J^{-1}), and b is the intercept (dimensionless). The difference in the decomposition mode for a solid-state reaction is the most common cause for the appearance of the kinetic compensation effect [14]. According to Barrie [15], systematic errors in kinetic measurements can also lead to the kinetic compensation effect.

The kinetic compensation effect was extensively existed in biomass thermochemical conversion processes, for example, the pyrolysis of cellulose [16], pyrolysis of biomass [17], pyrolysis of torrefied biomass [18], gasification of biochar [19], gasification of biomass-coal blends [20], and combustion of woody biomass [21] (see **Table 1**). Some processes involve multiple stages, in which different reactions with different kinetic parameters occur. Therefore, various kinetic compensation effect expresses were presented to describe them. However, the study on the kinetic compensation effect in lignocellulosic biomass torrefaction is still missing.

Table 1. Research examples of kinetic compensation effect in biomass thermochemical conversion process [a]

Biomass thermochemical conversion process	Kinetic compensation effect	Reference
Co-gasification of biomass after hydrothermal treatment and coal	Co-pyrolysis: $\ln k_0 = 0.2340E_a - 4.3186$ Co-gasification of biomass-char and coal-char: $\ln k_0 = 0.1217E_a - 6.2181$	[20]
Pyrolysis of torrefied Eucalyptus clone	Conversion range 0.05 – 0.60: $\ln k_0 = 0.182E_a - 3.678$ Conversion range 0.60 – 0.70: $\ln k_0 = 0.207E_a - 7.809$ Conversion range 0.70 - 0.80: $\ln k_0 = 0.267E_a - 8.793$	[18]
Pyrolysis of cellulosic materials	$\ln k_0 = 0.1939E_a - 1.0484$	[17]
Pyrolysis of cellulose	$\ln k_0 = 0.1887E_a - 5.0533$	[16]
Gasification of Australian mallee wood pyrolysis biochar in H_2O	H_2 formation: $\ln k_0 = 0.1158E_a - 4.2986$ CO formation: $\ln k_0 = 0.1118E_a - 4.4195$	[19]
Combustion of wood and leaf samples	Thermal decomposition: $\ln k_0 = 0.2262E_a - 3.0334$ Char combustion: $\ln k_0 = 0.1727E_a - 2.5444$	[21]

[a] E_a is expressed in kJ mol^{-1} and k_0 is expressed in min^{-1}.

Thermodynamic analysis is fundamental in the development of the biomass conversion industry, facilitating the design and optimization of thermochemical conversion processes, and avoiding difficult measurements [22]. Some researches focused on the thermodynamic analyses of pyrolysis and gasification processes of torrefied biomass [23, 24]. However, only a few studies were found to be related to lignocellulosic biomass torrefaction. Kumar et al. [25] performed the exergy and energy analyses of biomass torrefaction, while focused on the energy lost and wasted in the torrefaction system. Detcheberry et al. [26] modeled the thermodynamic behavior of the condensation of a gaseous effluent from wood torrefaction. Calusen et al. [27] investigated the total energy efficiencies of biomass gasification with integrated and external torrefaction. None of the above researchers calculated the thermodynamic parameters of the torrefaction process.

Therefore, in this paper, the torrefaction kinetics of lignocellulosic biomass was investigated with special attention to the kinetic compensation effect between the kinetic parameters, and the changes in thermodynamic parameters were calculated and analyzed according to the obtained optimal kinetic parameters.

2 Materials and experiments

The lignocellulosic biomass sample (pinewood) was collected from Suzhou City, Anhui Province, P. R. China. After grinding, sieving and drying, the sample with the diameters less than 0.5 mm was prepared for its physicochemical characterization and torrefaction kinetic tests. The proximate, elemental, compositional analyses of the sample were performed according to the methods recommended in our previous paper [28]. The lower heating value (LHV) of the sample was measured in an oxygen bomb calorimeter (XRY-1B, Shanghai Changji Geological Instruments Co., Ltd., China). The physicochemical analysis results of the pinewood sample were listed in **Table 2**.

Table 2. Physicochemical analyses of pinewood sample

Item	Value	Test standard
Proximate analysis (on dry basis)		
Ash (wt.%)	0.6	ASTM D1102
Volatile matter (wt.%)	83.1	ASTM E872-82
Fixed carbon (wt.%)	16.3	Calculated by difference
Ultimate analysis (on dry ash-free basis)		
C (wt.%)	45.83	● ASTM D8056-18
H (wt.%)	6.35	● The O content is calculated by difference.
O (wt.%) [a]	47.51	
N (wt.%)	0.31	
Energy content analysis (on dry basis)		
LHV (MJ kg^{-1})	17.1	ASTM D8056-18
Compositional analysis (on dry basis)		
Cellulose (wt.%)	42.2	● NREL/TP-510-42618 (from National
Hemicellulose (wt.%)	16.6	Renewable Energy Laboratory, USA)
Lignin (wt.%)	25.6	
Extractives (wt.%)	15.6	

The torrefaction kinetics of the lignocellulosic biomass sample was measured by thermogravimetric analysis (TGA), which is a thermal analysis technique used to determine an organic solid waste's thermal decomposition characterization by monitoring the mass change over time and/or temperature [29]. In this study, TGA under inert nitrogen environment was selected to perform the torrefaction kinetic process of the sample. The heating program used in

this study included two dynamic and two isothermal heating steps: (1) the sample was heated to 105 °C from room temperature with the heating rate of 25 °C min^{-1}, (2) then the temperature upheld at 105 °C for 10 min to remove the moisture contained in the sample; (3) the sample was heated to the specified torrefaction temperatures (220, 250, 265, 280, and 295 °C) with the heating rate of 25 °C min^{-1}; (4) afterwards, the specified torrefaction temperature maintained for 5 h. Detailed information about TGA was listed in **Table3**. The experimental data set at 220, 250 and 280 °C has been used for kinetic analysis, while the experimental data at 265 and 295 °C has been employed for validation. Every TGA experiment repeated three times, and the average values were used for kinetic analysis. The experimental data of the isothermal step at specified torrefaction temperature was used for latter kinetic analysis.

The schematic diagram of the sample processing, experiments and calculations was presented in **Figure 1**.

Table 3. Information about TGA for biomass torrefaction

Item	**Information**
Apparatus	Thermogravimetric analyzer (TGA 7, Perkin Elmer, Inc., USA)
Isothermal measurement temperatures	220 °C; 250 °C; 265 °C; 280 °C; 295 °C
Atmosphere	Nitrogen with high purity (>99.9 vol. %) (purge flow rate: 60 mL min^{-1})
Test standard	ASTM E2402 – 19: Standard Test Method for Mass Loss, Residue, and Temperature Measurement Validation of Thermogravimetric Analyzers

Sample mass at one test	~ 4.5 mg

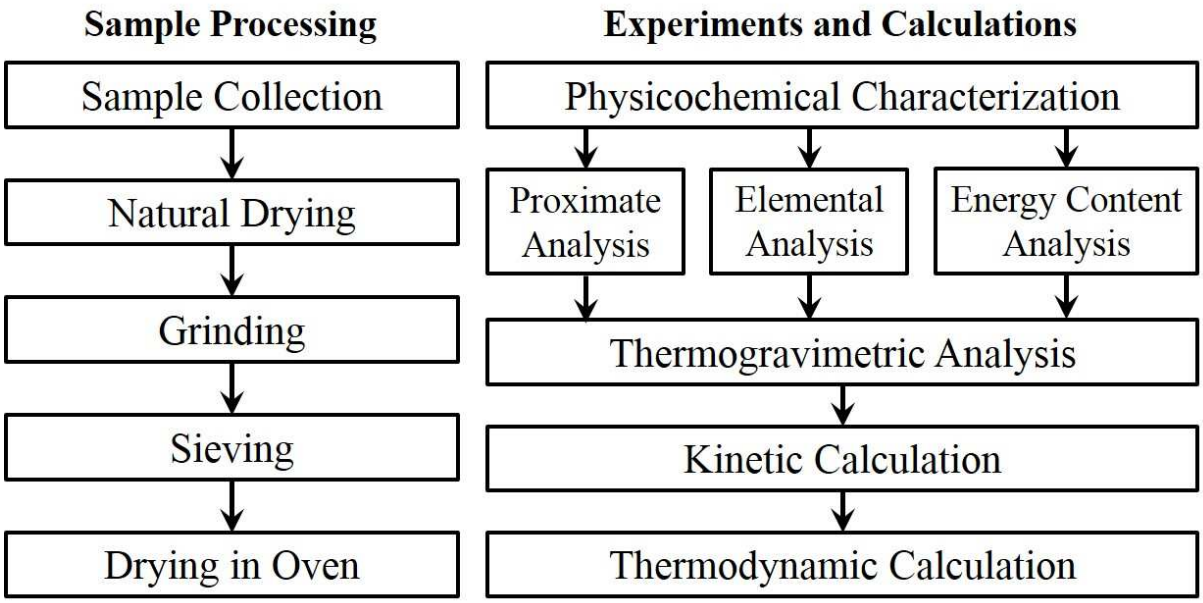

Figure 1. Schematic diagram of sample processing, experiments and calculations in this study

3 Torrefaction model and data processing method

In literature, some kinetic models were proposed to describe biomass torrefaction kinetics, such as the two-step reaction model [30], distributed activation energy model (DAEM) [31], and global reaction model [11]. The two-step reaction model assumes two-step sequential reactions: woody biomass decomposes into the volatile and intermediate product, then the intermediate product further decomposes into the volatile and torrefied biomass. The two-step reaction model involves the formation and decomposition of the intermediate product, which cannot be accurately quantified using existing measuring techniques. Therefore, the model has not been verified yet. The DAEM assumes an infinite number of parallel reactions with the same pre-exponential factor and different activation energies which can be represented by a continuous distribution function. For the DAEM, the assumption of the activation energies with

a continuous distribution function is over-idealized, and the differences between the assumed and the real activation energy distribution are substantial. The DAEM equation has complex mathematical structure leading to difficulties in parameter estimation [32]. And the global reaction kinetic model assumes that biomass decomposes into the torrefaction volatile and solid torrefied product and uses two kinetic parameters, including the pre-exponential factor and activation energy to describe the kinetic process of biomass torrefaction. Compared with the two-step kinetic model and DAEM, the global reaction kinetic model is simple and easy to use, and its accuracy is good enough in describing biomass torrefaction kinetics. In this study, the global reaction kinetic model was considered in the kinetic analysis of pinewood isothermal torrefaction:

$$\begin{cases} \mathrm{d}\dfrac{v(t)}{v_f}\Big/\mathrm{d}t = k_0 \cdot \exp\left(-\dfrac{E_a}{R(T+273.15)}\right)\cdot\left[1-\dfrac{v(t)}{v_f}\right] \\ t=0,\ \dfrac{v(t)}{v_f}=0 \end{cases} \tag{3}$$

where $v(t)$ is the amount of releasing volatiles (mg) at the time t and v_f is the total amount of releasing volatiles (mg).

Integration of Equation (3) resulted in the following equation:

$$\frac{v(t)}{v_f} = 1-\exp\left[-k_0 \cdot \exp\left(-\frac{E_a}{R(T+273.15)}\right)\cdot t\right] \tag{4}$$

To determine the parameters (including k_0 and E_a) in the above model, the following objective function was established:

$$\mathrm{SSE}(k_0, E_a) = \sum_{i=1}^{n_d}\left\{\left[\frac{v(t_i)}{v_f}\right]_{\mathrm{exp}}^2 - \left[\frac{v(t_i)}{v_f}\right]_{\mathrm{cal}}^2\right\} \tag{5}$$

where SSE is the sum of squares of errors between experimental data and data calculated from Equation (4), the subscript i represents the i-th data point, n_d is the number of data points, the

subscripts exp and cal denote the experimental data and the data calculated from the model. The optimal kinetic parameters minimizing the above objective function is the resulting ones.

The goodness-of-fit of the kinetic model for describing the experimental data was evaluated by two statistical measures: the coefficient of determination (R^2) and the variation coefficient (VC). The variation coefficient is defined as follows:

$$\mathrm{VC}\ /\ \% = \frac{\sqrt{\mathrm{SSE} \big/ \left(n_d - p\right)}}{\mathrm{mean}\left(\left[\frac{v(t_i)}{v_f}\right]_{\mathrm{exp}}\right)} \times 100 \tag{6}$$

where 'mean' denotes the mean value, p is the number of parameters, and σ represents the standard deviation. The closer R^2 is to 1, the more closely the model fits the sample data. VC is a measure of relative variability, which is the ratio of the standard deviation to the mean.

In this work, all numerical calculations were carried out in the MATLAB software environment. The block diagram and corresponding pseudo-code for the numerical calculations concerned in this work were summarized in **Figure 2**.

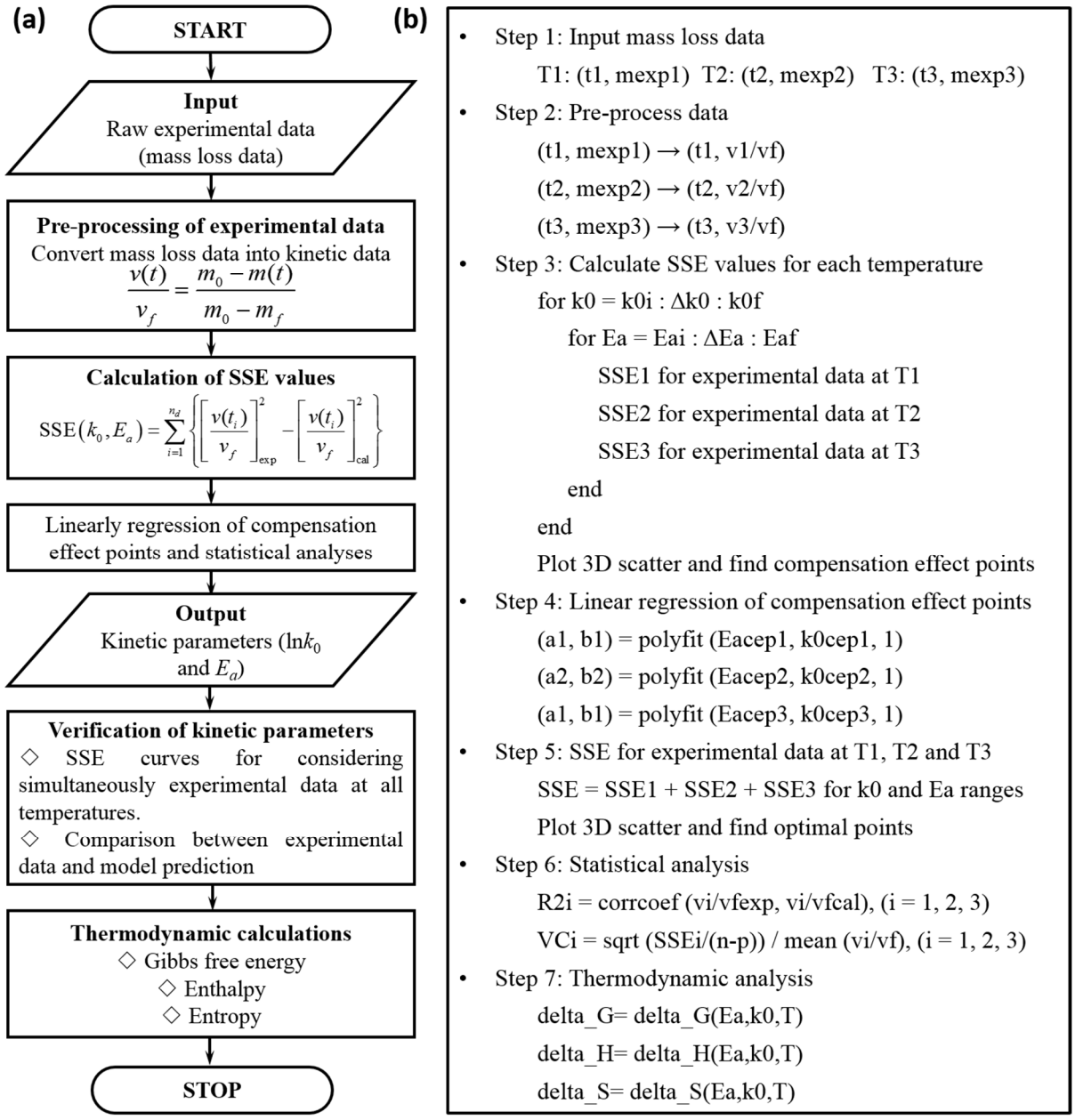

Figure 2. (a) Block diagram and (b) pseudo-code for numerical calculations

4 Results and discussion

The values of $v(t)$ and v_f can be calculated using TGA data:

$$\frac{v(t)}{v_f} = \frac{m_0 - m(t)}{m_0 - m_f} \tag{7}$$

where m_0 (mg), $m(t)$ (mg) and m_f (mg) are the initial mass, the mass of torrefaction solid residual at time t, and the final mass of torrefaction solid residual, respectively. In the literature

[33], $\frac{v(t)}{v_f}$ was expressed as α, the degree of conversion, which ranged between 0 and 1. The final mass is a function of the torrefaction temperature and initial mass. The $\frac{v(t)}{v_f}$ values at various time for a specified torrefaction temperature were obtained from the m_0, $m(t)$ and m_f data at that temperature.

The processed experimental data of lignocellulosic biomass torrefaction at different temperatures of 220, 250 and 280 °C were shown in **Figure 3**, where it was obtained that higher temperatures resulted in the releasing of more torrefaction volatiles.

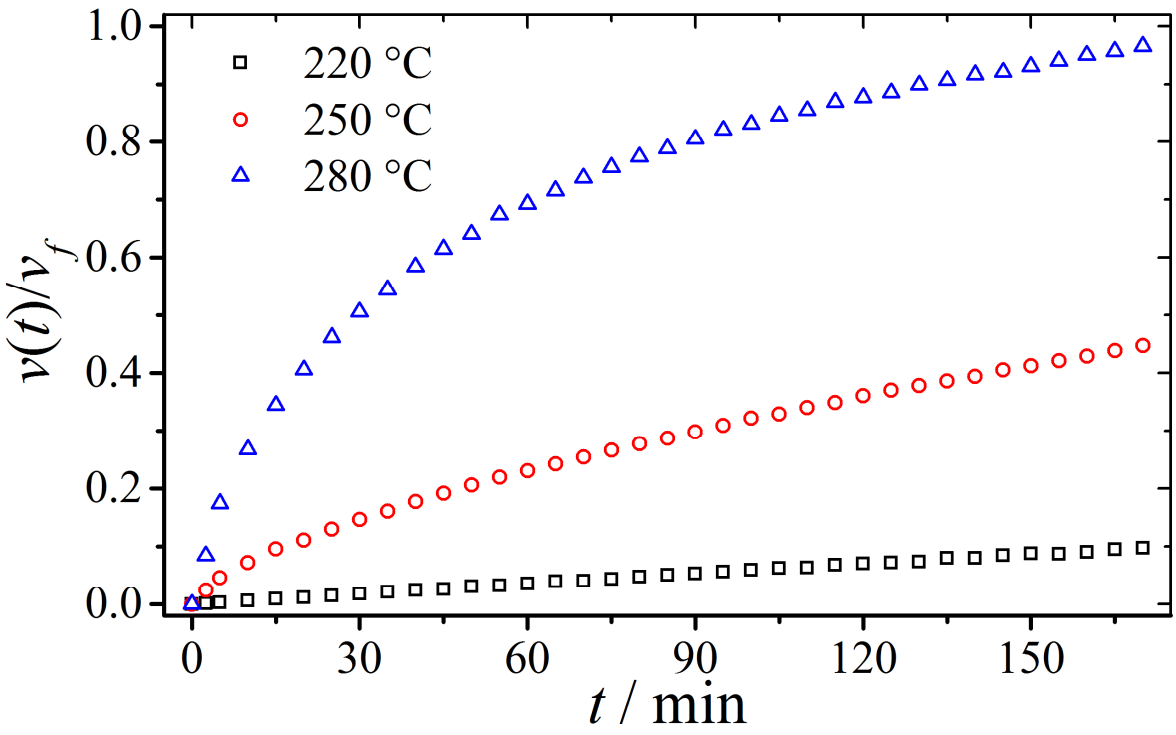

Figure 3. Processed experimental data of lignocellulosic biomass torrefaction at three temperatures of 220, 250 and 280 °C

To investigate the effect of lnk_0 and E_a on the results of SSE, the kinetic experimental data of lignocellulosic biomass torrefaction at 220, 250 and 280 °C were substituted into Equation

(4) and the SSE values for various lnk_0 (from 20 to 22 with interval of 0.2, k_0 in s^{-1}) and E_a (from 125 to 145 kJ mol^{-1} with interval of 0.01 kJ mol^{-1}) values (see **Figure 4**). To present the results more clearly, only those points whose SSE values are less than 0.04, 0.06 and 0.08 for 220, 250 and 280 °C were shown. It was found that many points could reach the minimum SSE value simultaneously, which indicated that many sets of lnk_0 and E_a could describe the experimental data at every temperature equally well.

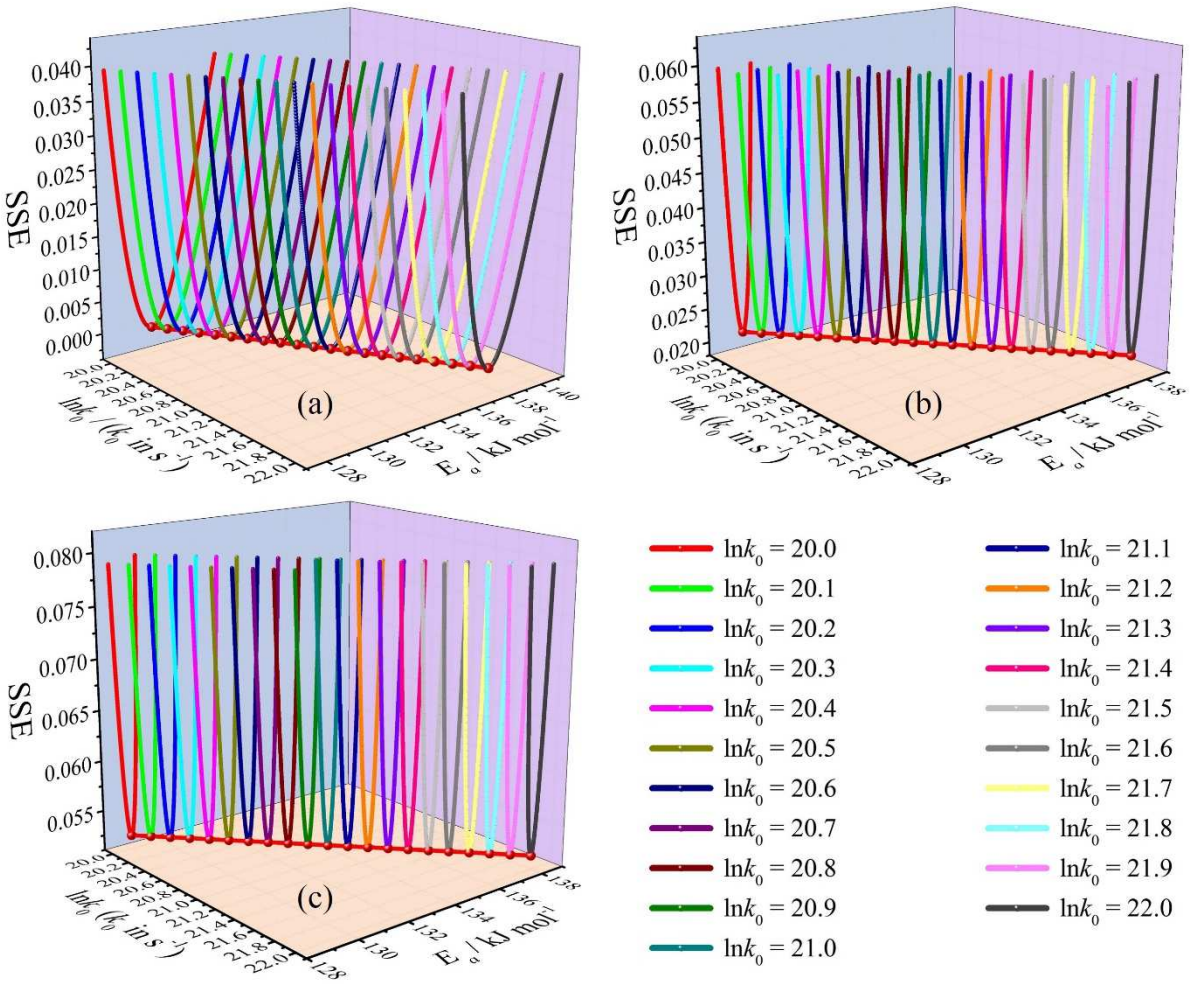

Figure 4. SSE curves with various lnk_0 and E_a values for fitting of experimental data at (a) 220 °C; (b) 250 °C; (c) 280 °C.

A perfect linear relationship between those sets of lnk_0 and E_a for each temperature

were found (**Figure 5**), which indicated that they followed the kinetic compensation effect. The linear regression lines of kinetic compensation effect points for three temperatures were observed to intersect at one particular point, where $\ln k_0$ = 21.08 and E_a = 133.75 kJ mol^{-1}, respectively. The linear regression results of compensation effect points for different temperatures were listed in **Table 4**. And the values of $1000/R/(T_t+273.15)$ were also included in **Table 4**. From the results included in **Table 4**, it was obtained that the values of a and $1000/R/(T_t+273.15)$ were very close for all cases, which was consistent with the isokinetic relationship extensively existed in many chemical reactions: $\ln A_j = \ln k_{\text{iso}} + \dfrac{1000E_j}{R(T_{\text{iso}}+273.15)}$ (E_j is expressed in kJ mol^{-1}) [34].

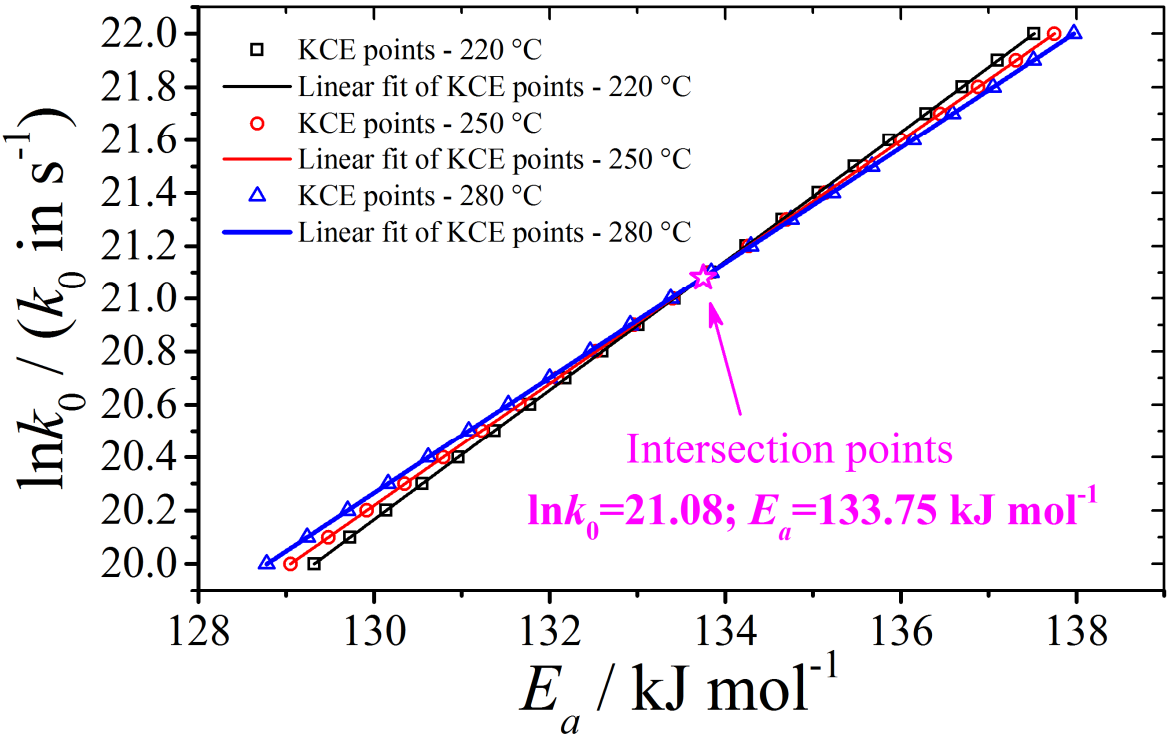

Figure 5. Linear regression of kinetic compensation effect points for three temperatures (KCE in figure represents kinetic compensation effect)

Table 4. Linear regression results of compensation effect points

T_t / °C	Compensation effect parameters			1000/R/(T_t+273.15) / mol kJ^{-1}
	a / mol kJ^{-1}	b	R$^{2\,a}$	
220	0.2440	-11.5534	1.000	0.2439
250	0.2298	-9.6600	1.000	0.2299
280	0.2176	-8.0276	1.000	0.2174

The SSE values for various lnk_0 and E_a with simultaneously considering the experimental data at all temperatures were computed and shown in **Figure 6**, where it was seen that there was an optimal point minimizing the SSE value. The lnk_0 and E_a values corresponding to the optimal point were 21.05 and 133.79 kJ mol^{-1}, respectively, which were very close to those values corresponding to the intersection point of the compensation effect lines for different temperatures.

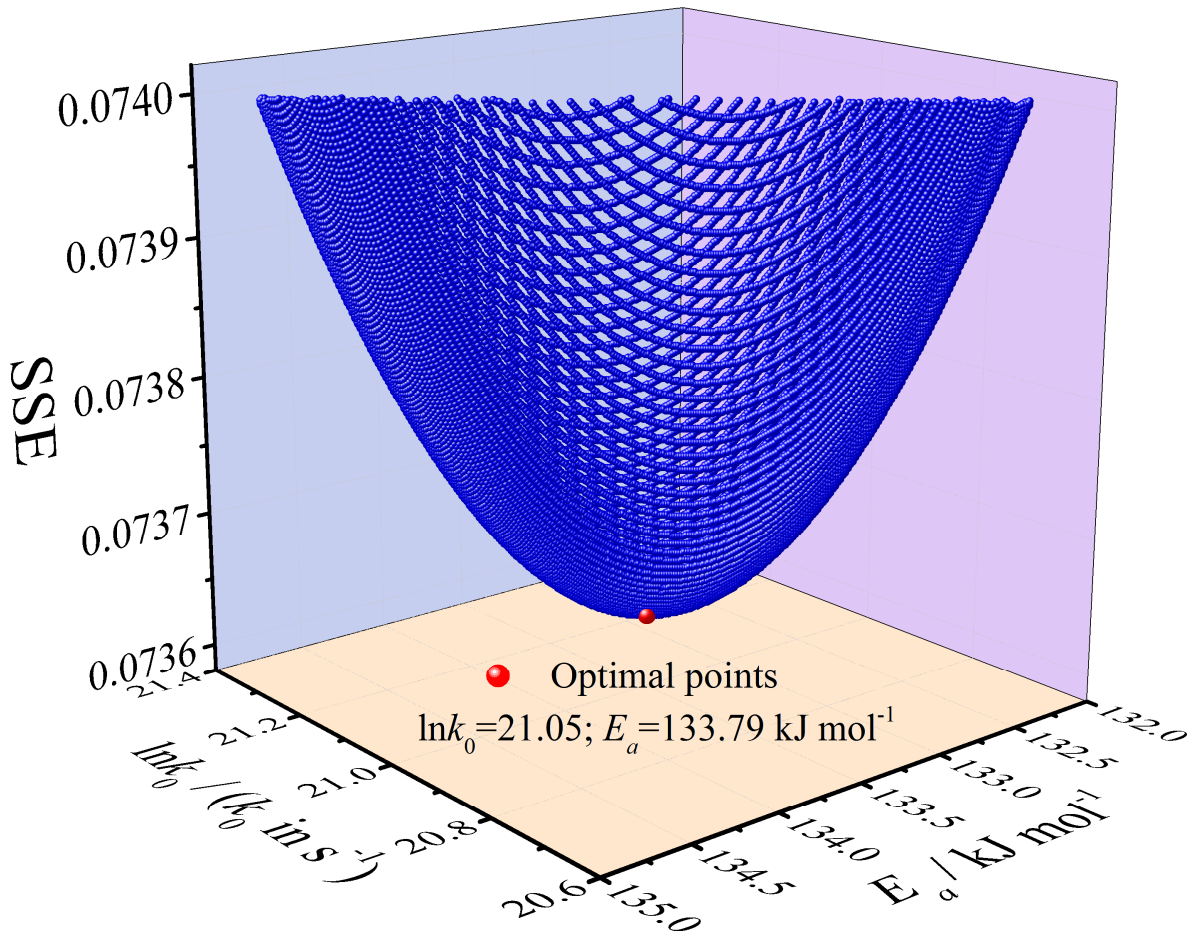

Figure 6. SSE values for various $\ln k_0$ and E_a values with considering experimental data at all temperatures simultaneously

Based on the optimal parameters ($\ln k_0$ = 21.08 and E_a = 133.75 kJ mol^{-1}) obtained from the kinetic compensation effect analysis, the prediction was calculated from Equation (4) for different temperatures, and the corresponding statistical analyses were performed (see **Figure 7**). It was observed that the optimal parameters could describe the experimental data at different temperatures very well ($R^2 > 0.98$ and VC < 7.45%).

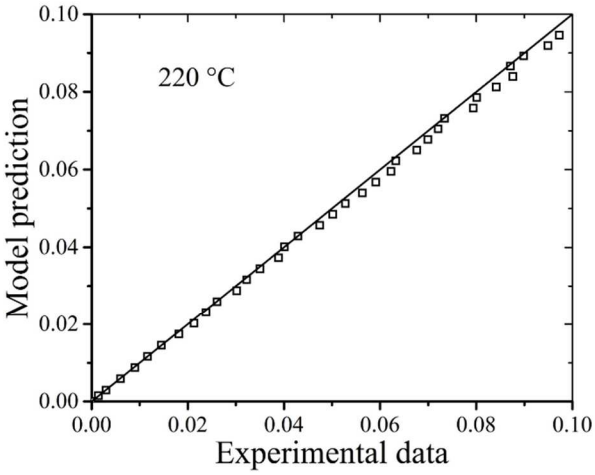

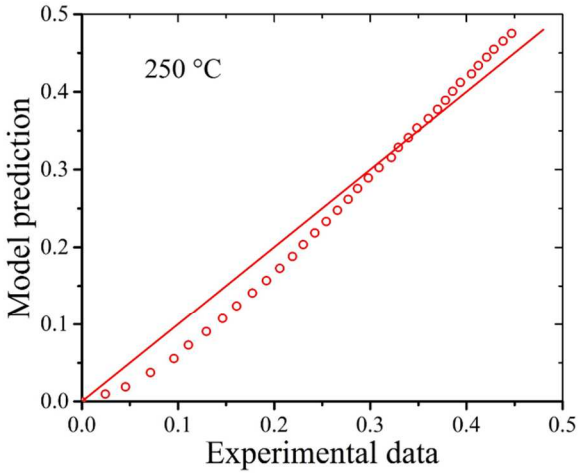

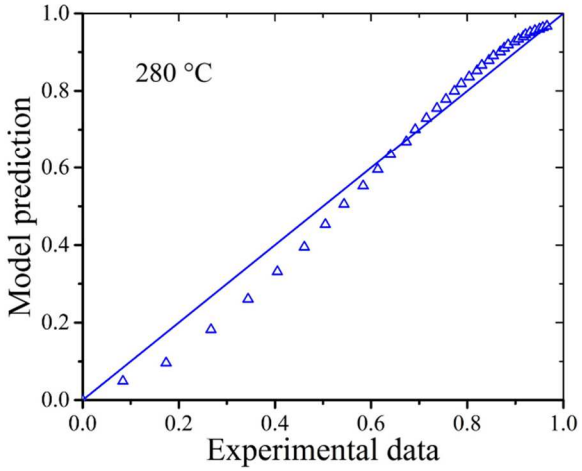

Statistical analysis results

T_t / °C	R^2	VC / %
220	0.992	3.712
250	0.982	7.430
280	0.983	5.676

Figure 7. Comparison between experimental data and model prediction at 220, 250 and 280 °C

To verify the accuracy of the model coupled with the optimal kinetic parameters at the extra temperature, the comparison between the experimental data at interpolated and extrapolated temperatures of 265 and 295 °C, and the corresponding model prediction was shown in **Figure 8**. It could be seen from **Figure 8** that the model could predict the experimental data well, which indicated the reliability of the method for the determination of the kinetic parameters and the accuracy of the resulting kinetic parameters. Based on the reaction order model with the optimal kinetic parameters, the $v(t)/v_f$ *vs.* t curves at an extra temperature of 235 °C could be predicted and also included in **Figure 8**.

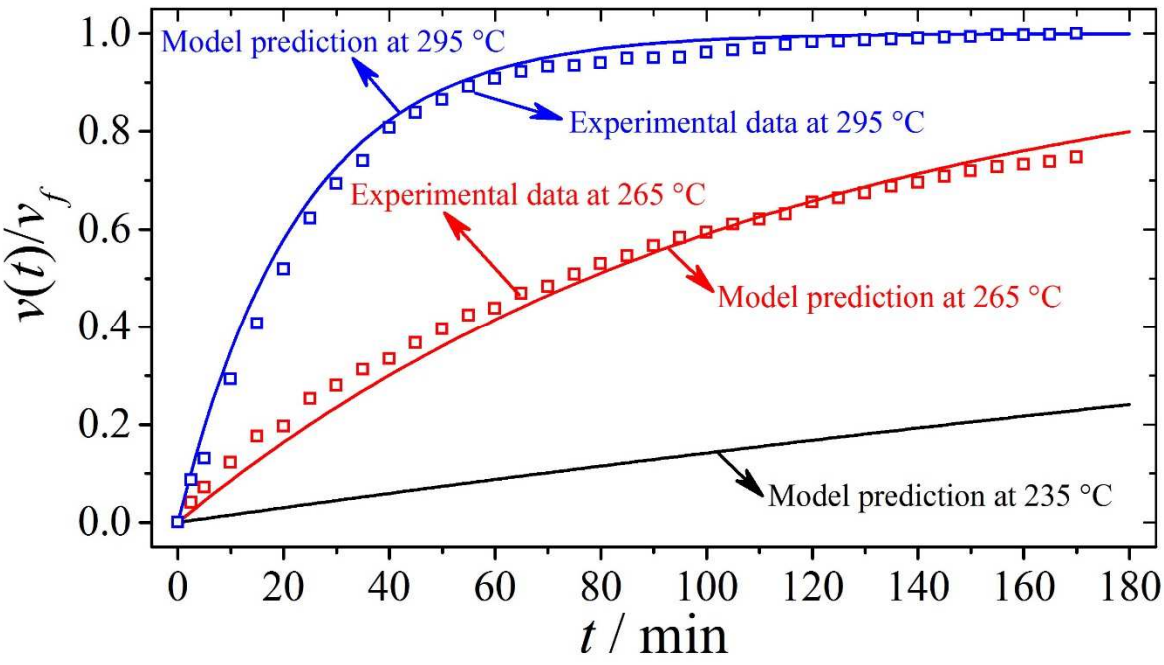

Figure 8. Validation of $v(t)/v_f$ at 265 and 295 °C and prediction of $v(t)/v_f$ at 235 °C

Pinewood contains three bio-polymer components: cellulose, hemicellulose, and lignin. Those components decompose over different temperature range [35]: hemicellulose decomposes at a relatively low-temperature range of 200 – 350 °C because of its branched structure, cellulose decomposes at the moderate temperature range of 325 – 400 °C, while lignin decomposes at a wide temperature range of 250 – 500 °C [36, 37]. Therefore, under torrefaction conditions (200 – 300 °C), the reactions occurring during torrefaction include the decomposition of hemicellulose and lignin, with small contribution from the latter [38]. The relatively small activation energy value for the isothermal torrefaction of pinewood at the temperature range of 220 - 295 °C attributed to the decomposition of hemicellulose contained in pinewood.

The activation energy of pinewood torrefaction was close to that of beech wood torrefaction (122.9 kJ mol^{-1}) [11]. Awang et al. [39] performed the torrefaction of *Leucaena Leucocephala* and obtained its activation energy of 42.3 kJ mol^{-1} using the Coats-Redfern method. The Coats-Redfern kinetic method used the oversimplified approximation of the

temperature integral, which would lead to a significant system error in the determination of the activation energy [40].

The above kinetic analysis of pinewood torrefaction can calculate the activation energy required for the torrefaction reaction to proceed. However, it gives no information about conditions once the torrefaction reaction equilibrates. Thermodynamic analysis can provide information regarding the equilibrium conditions of solid torrefaction product (torrefied biomass) after the torrefaction reaction takes place [41]. Therefore, the thermodynamic analysis of pinewood torrefaction was carried out and the corresponding results and discussion were listed as follows.

Based on the activation energy and pre-exponential factor, the thermodynamic parameters of activation (including Gibbs free energy, enthalpy, and entropy) can be calculated from the Eyring Theory [42-45]:

$$\Delta G^* = E_a + R \cdot (T + 273.15) \cdot \ln\left(\frac{\kappa_B \cdot (T + 273.15)}{h \cdot k_0}\right) \quad (8)$$

$$\Delta H^* = E_a - R \cdot (T + 273.15) \quad (9)$$

$$\Delta S^* = \frac{\Delta H^* - \Delta G^*}{T + 273.15} \quad (10)$$

where ΔG^* (J mol^{-1}), ΔH^* (J mol^{-1}) and ΔS^* (J mol^{-1} °C^{-1}) are the changes in Gibbs free energy, enthalpy, and entropy of activation, respectively, κ_B represents the Boltzmann constant (1.381×10^{-23} J K^{-1}), and h is the Plank constant (6.626×10^{-34} J s^{-1}).

Table 5 listed the thermodynamic parameter values for lignocellulosic biomass torrefaction at different temperatures. The changes in Gibbs free energy represent the potential work and the spontaneity of a chemical process [46]. The ΔG^* values of pinewood torrefaction slightly increased with increasing temperature, which indicated that the spontaneity in the torrefaction decomposition reaction increased at higher temperatures. The changes in enthalpy

represent the difference in energy between reactant (raw pinewood) and products (torrefaction volatile and solid torrefied biomass) and ascertain that a chemical reaction process will be endothermic or exothermic [47]. The positive values of ΔH^* for lignocellulosic biomass torrefaction indicated that energy was required for the decomposition reaction during torrefaction. There was a slight difference in ΔH^* for lignocellulosic biomass torrefaction at different temperatures, which showed that similar energy in the decomposition reaction during torrefaction at different temperatures. The changes in entropy can be considered as the disorder degree of a chemical reaction [48]. The ΔS^* values of pinewood torrefaction showed negative values and increased with increasing temperature, which indicated that the torrefaction decomposition reaction at higher temperatures was more activated.

To the best of our knowledge, there is no thermodynamic reference parameter result that stands for the isothermal torrefaction of biomass. However, there existed some thermodynamic analysis results for the nonisothermal pyrolysis of biomass [49-51], which were crucially different from each other. For example, Mishra et al. [49] calculated the average thermodynamic parameter values for *Phyllanthus emblica* pyrolysis: ΔG^* = 215 kJ mol^{-1}, ΔH^* = 182 kJ mol^{-1}, ΔS^* = -72 J mol^{-1} K^{-1}, and while Singh et al. [51] obtained the average thermodynamic parameter values for banana leaves biomass pyrolysis: ΔG^* = 81 kJ mol^{-1}, ΔH^* = 64 kJ mol^{-1}, ΔS^* = -63 J mol^{-1} K^{-1}. The thermodynamic parameter values of the pyrolysis of biomass feedstocks could depend on material nature, pyrolysis conditions, and thermodynamic calculation method.

Based on the above analyses, it can be stated that the kinetics is related to the reactivity of the decomposition reaction of pinewood torrefaction (reaction rate, pathway and activation energy), while thermodynamics is related to several thermodynamic parameters, whose values do not depend on the torrefaction decomposition reaction pathway. According to the thermodynamic analysis, the heat required for decomposition reaction during torrefaction under

different torrefaction temperatures can be further calculated and can be used to estimate the heat and exergy efficiencies of a torrefaction system together with energy input and output, and system heat loss [52, 53].

Table 5. Thermodynamic parameter values for lignocellulosic biomass torrefaction at different temperatures

T / °C	ΔG^* / kJ mol^{-1}	ΔH^* / kJ mol^{-1}	ΔS^* / J mol^{-1} °C^{-1}
220	170.165	129.650	-82.156
235	171.399	129.525	-82.405
250	172.637	129.400	-82.647
265	173.879	129.276	-82.882
280	175.124	129.151	-83.111
295	176.372	129.026	-83.333

5 **Conclusion**

Many sets of k_0 and E_a could describe the experimental data at each temperature equally well and excellently satisfied the kinetic compensation effect relationship. The linear regression lines of those kinetic compensation effect points intersected at one point ($\ln k_0$ = 21.08 and E_a = 133.75 kJ mol^{-1}), which could minimize the SSE values with considering experimental data at all temperatures simultaneously. This paper provided a proven method for determining the kinetic parameters based on the kinetic compensation effect. When the torrefaction temperature increased from 220 to 295 °C, the ΔG^* values increased from 170.1 to 176.4 kJ mol-1, the ΔH^* values slightly decreased from 129.7 to 129.0 kJ mol^{-1}, the ΔS^* values changed from -82.1 to -83.3 J mol^{-1} °C^{-1}.

Acknowledgements

Financial support from CAS Key Laboratory of Renewable Energy (Project No. Y807k91001) is greatly acknowledged. Mr. Laipeng Luo, a junior student from School of Agriculture and Biology, Shanghai Jiao Tong University, P. R. China, is greatly acknowledged for his help in thermodynamic calculation.

References

[1] Barskov S, Zappi M, Buchireddy P, Dufreche S, Guillory J, Gang D, et al. Torrefaction of biomass: A review of production methods for biocoal from cultured and waste lignocellulosic feedstocks. Renewable Energy. 2019;142:624-42.

[2] Baruah J, Nath BK, Sharma R, Kumar S, Deka RC, Baruah DC, et al. Recent trends in the pretreatment of lignocellulosic biomass for value-added products. Frontiers in Energy Research. 2018;6:Article 141.

[3] Bhatia SK, Jagtap SS, Bedekar AA, Bhatia RK, Patel AK, Pant D, et al. Recent developments in pretreatment technologies on lignocellulosic biomass: Effect of key parameters, technological improvements, and challenges. Bioresource Technology. 2020;300:122724.

[4] Cahyanti MN, Doddapaneni TRKC, Kikas T. Biomass torrefaction: An overview on process parameters, economic and environmental aspects and recent advancements. Bioresource Technology. 2020;301:122737.

[5] Meng J, Park J, Tilotta D, Park S. The effect of torrefaction on the chemistry of fast-pyrolysis bio-oil. Bioresource Technology. 2012;111:439-46.

[6] Mamvura TA, Danha G. Biomass torrefaction as an emerging technology to aid in energy production. Heliyon. 2020;6(3):e03531.

[7] Commandré JM, Leboeuf A. Volatile yields and solid grindability after torrefaction of

various biomass types. Environmental Progress & Sustainable Energy. 2015;34(4):1180-6.

[8] He Q, Ding L, Gong Y, Li W, Wei J, Yu G. Effect of torrefaction on pinewood pyrolysis kinetics and thermal behavior using thermogravimetric analysis. Bioresource Technology. 2019;280:104-11.

[9] Szufa S, Dzikuć M, Adrian L, Piersa P, Romanowska-Duda Z, Lewandowska W, et al. Torrefaction of oat straw to use as solid biofuel, an additive to organic fertilizers for agriculture purposes and activated carbon-TGA analysis, kinetics. Energies. 2020;13(8):2064.

[10] Ribeiro JMC, Godina R, Matias JCO, Nunes LJR. Future perspectives of biomass torrefaction: Review of the current state-of-the-art and research development. Sustainability (Switzerland). 2018;10(7):2323.

[11] Duan H, Zhang Z, Rahman MM, Guo X, Zhang X, Cai J. Insight into torrefaction of woody biomass: Kinetic modeling using pattern search method. Energy. 2020;201:117648.

[12] Luo L, Guo X, Zhang Z, Chai M, Rahman MM, Zhang X, et al. Insight into pyrolysis kinetics of lignocellulosic biomass: Isoconversional kinetic analysis by the modified Friedman method. Energy & Fuels. 2020;34(4):4874-81.

[13] L'vov BV, Galwey AK. Interpretation of the kinetic compensation effect in heterogeneous reactions: thermochemical approach. International Reviews in Physical Chemistry. 2013;32(4):515-57.

[14] L'Vov B. Chapter 12. The Kinetic Compensation Effect. Thermal Decomposition of Solids and Melts: Springer, Dordrecht; 2007. p. 139-41.

[15] Barrie PJ. The mathematical origins of the kinetic compensation effect: 2. The effect of systematic errors. Physical Chemistry Chemical Physics. 2012;14(1):327-36.

[16] Xu D, Chai M, Dong Z, Rahman MM, Yu X, Cai J. Kinetic compensation effect in logistic distributed activation energy model for lignocellulosic biomass pyrolysis. Bioresource Technology. 2018;265:139-45.

[17] Agrawal RK. Compensation effect in the pyrolysis of cellulosic materials. Thermochimica Acta. 1985;90:347-51.

[18] Doddapaneni TRKC, Konttinen J, Hukka TI, Moilanen A. Influence of torrefaction pretreatment on the pyrolysis of Eucalyptus clone: A study on kinetics, reaction mechanism and heat flow. Industrial Crops and Products. 2016;92:244-54.

[19] Akhtar MA, Zhang S, Li C-Z. Mechanistic insights into the kinetic compensation effects during the gasification of biochar in H_2O. Fuel. 2019;255:115839.

[20] Wei J, Song X, Guo Q, Ding L, Yoshikawa K, Yu G. Reactivity, synergy, and kinetics analysis of CO_2 co-pyrolysis/co-gasification of biomass after hydrothermal treatment and coal blends. Energy & Fuels. 2020;34(1):294-303.

[21] Liu N, Wang B, Fan W. Kinetic compensation effect in the thermal decomposition of biomass in air atmosphere. Fire Safety Science. 2003;7:581-92.

[22] Kumar M, Shukla SK, Upadhyay SN, Mishra PK. Analysis of thermal degradation of banana (Musa balbisiana) trunk biomass waste using iso-conversional models. Bioresource Technology. 2020;310:123393.

[23] Singh S, Prasad Chakraborty J, Kumar Mondal M. Intrinsic kinetics, thermodynamic parameters and reaction mechanism of non-isothermal degradation of torrefied *Acacia nilotica* using isoconversional methods. Fuel. 2020;259:116263.

[24] Clausen LR. Integrated torrefaction vs. external torrefaction - A thermodynamic analysis for the case of a thermochemical biorefinery. Energy. 2014;77:597-607.

[25] Kumar MS, Singh A, Jithu VP, Murali RA, Revuru A, Das A. Thermodynamic analysis of torrefaction process. International Journal of Renewable Energy Research. 2016;6(1):245-9.

[26] Detcheberry M, Destrac P, Massebeuf S, Baudouin O, Gerbaud V, Condoret JS, et al. Thermodynamic modeling of the condensable fraction of a gaseous effluent from lignocellulosic biomass torrefaction. Fluid Phase Equilibria. 2016;409:242-55.

[27] Clausen LR. Integrated torrefaction vs. external torrefaction – A thermodynamic analysis for the case of a thermochemical biorefinery. Energy. 2014;77:597-607.

[28] Cai J, He Y, Yu X, Banks SW, Yang Y, Zhang X, et al. Review of physicochemical properties and analytical characterization of lignocellulosic biomass. Renewable and Sustainable Energy Reviews. 2017;76:309-22.

[29] Cai J, Xu D, Dong Z, Yu X, Yang Y, Banks SW, et al. Processing thermogravimetric analysis data for isoconversional kinetic analysis of lignocellulosic biomass pyrolysis: Case study of corn stalk. Renewable and Sustainable Energy Reviews. 2018;82:2705-15.

[30] Prins MJ, Ptasinski KJ, Janssen FJJG. Torrefaction of wood: Part 1. Weight loss kinetics. Journal of Analytical and Applied Pyrolysis. 2006;77(1):28-34.

[31] Sarvaramini A, Assima GP, Larachi F. Dry torrefaction of biomass – Torrefied products and torrefaction kinetics using the distributed activation energy model. Chemical Engineering Journal. 2013;229:498-507.

[32] Cai J, Wu W, Liu R. An overview of distributed activation energy model and its application in the pyrolysis of lignocellulosic biomass. Renewable and Sustainable Energy Reviews. 2014;36:236-46.

[33] Li X, Mei Q, Dai X, Ding G. Effect of anaerobic digestion on sequential pyrolysis kinetics of organic solid wastes using thermogravimetric analysis and distributed activation energy model. Bioresource Technology. 2017;227:297-307.

[34] Barrie PJ. The mathematical origins of the kinetic compensation effect: 1. The effect of random experimental errors. Physical Chemistry Chemical Physics. 2012;14(1):318-26.

[35] Chen W-H, Wang C-W, Ong HC, Show PL, Hsieh T-H. Torrefaction, pyrolysis and two-stage thermodegradation of hemicellulose, cellulose and lignin. Fuel. 2019;258:116168.

[36] Yang H, Yan R, Chen H, Lee DH, Zheng C. Characteristics of hemicellulose, cellulose and lignin pyrolysis. Fuel. 2007;86(12):1781-8.

[37] Balat M. Mechanisms of Thermochemical Biomass Conversion Processes. Part 1: Reactions of Pyrolysis. Energy Sources, Part A: Recovery, Utilization, and Environmental Effects. 2008;30(7):620-35.

[38] Kan T, Strezov V, Evans TJ. Lignocellulosic biomass pyrolysis: A review of product properties and effects of pyrolysis parameters. Renewable and Sustainable Energy Reviews. 2016;57:1126-40.

[39] Awang AN, Mohamed AR, Mohd Salleh NH, Hoo PY, Kasim NN. Torrefaction of Leucaena Leucocephala under isothermal conditions using the Coats–Redfern method: kinetics and surface morphological analysis. Reaction Kinetics, Mechanisms and Catalysis. 2019;128(2):663-80.

[40] Vyazovkin S, Burnham AK, Criado JM, Pérez-Maqueda LA, Popescu C, Sbirrazzuoli N. ICTAC Kinetics Committee recommendations for performing kinetic computations on thermal analysis data. Thermochimica Acta. 2011;520(1):1-19.

[41] Sieniutycz S. Chapter 8 - Thermodynamics and Optimization of Practical Processes. In: Sieniutycz S, editor. Thermodynamic Approaches in Engineering Systems. Amsterdam: Elsevier; 2016. p. 347-420.

[42] Kim YS, Kim YS, Kim SH. Investigation of thermodynamic parameters in the thermal decomposition of plastic waste−waste lube oil compounds. Environmental Science & Technology. 2010;44(13):5313-7.

[43] Mumbach GD, Alves JLF, Da Silva JCG, De Sena RF, Marangoni C, Machado RAF, et al. Thermal investigation of plastic solid waste pyrolysis via the deconvolution technique using the asymmetric double sigmoidal function: Determination of the kinetic triplet, thermodynamic parameters, thermal lifetime and pyrolytic oil composition for clean energy recovery. Energy Conversion and Management. 2019;200:112031.

[44] Alves JLF, Da Silva JCG, da Silva Filho VF, Alves RF, Ahmad MS, Ahmad MS, et al.

Bioenergy potential of red macroalgae Gelidium floridanum by pyrolysis: Evaluation of kinetic triplet and thermodynamics parameters. Bioresource Technology. 2019;291:121892.

[45] Alves JLF, da Silva JCG, da Silva Filho VF, Alves RF, de Araujo Galdino WV, De Sena RF. Kinetics and thermodynamics parameters evaluation of pyrolysis of invasive aquatic macrophytes to determine their bioenergy potentials. Biomass and Bioenergy. 2019;121:28-40.

[46] Khan AS, Man Z, Bustam MA, Kait CF, Ullah Z, Nasrullah A, et al. Kinetics and thermodynamic parameters of ionic liquid pretreated rubber wood biomass. Journal of Molecular Liquids. 2016;223:754-62.

[47] Yuan X, He T, Cao H, Yuan Q. Cattle manure pyrolysis process: Kinetic and thermodynamic analysis with isoconversional methods. Renewable Energy. 2017;107:489-96.

[48] Sinha D. Entropy changes in a thermodynamic process under potential gradients. Physica A: Statistical Mechanics and its Applications. 2014;416:676-83.

[49] Mishra RK, Mohanty K. Kinetic analysis and pyrolysis behaviour of waste biomass towards its bioenergy potential. Bioresource Technology. 2020;311:123480.

[50] Rasool T, Kumar S. Kinetic and thermodynamic evaluation of pyrolysis of plant biomass using TGA. Materials Today: Proceedings. 2020;21:2087-95.

[51] Singh RK, Pandey D, Patil T, Sawarkar AN. Pyrolysis of banana leaves biomass: Physico-chemical characterization, thermal decomposition behavior, kinetic and thermodynamic analyses. Bioresource Technology. 2020;310:123464.

[52] Saidur R, BoroumandJazi G, Mekhilef S, Mohammed HA. A review on exergy analysis of biomass based fuels. Renewable and Sustainable Energy Reviews. 2012;16(2):1217-22.

[53] Zhang X, Zeng R, Deng Q, Gu X, Liu H, He Y, et al. Energy, exergy and economic analysis of biomass and geothermal energy based CCHP system integrated with compressed air energy storage (CAES). Energy Conversion and Management. 2019;199:111953.